Accepted for publication in European Journal of Physics DOI: https://doi.org/10.1088/1361-6404/ab2afc

A Time-Energy Delayed-Choice Interference Experiment for the Undergraduate Laboratory

Jhonny Castrillón[1,2], Enrique J. Galvez[1], Boris A. Rodriguez[2], Omar Calderón-Losada[3]

[1] Department of Physics and Astronomy, Colgate University, Hamilton, NY, USA
[2] Instituto de Física, Universidad de Antioquia, Medellín, Colombia
[3] Quantum Optics Laboratory, Universidad de los Andes, Bogotá, Colombia

E-mail: egalvez@colgate.edu

Abstract. Laboratory experiments that illustrate the fundamentals of quantum physics are powerful teaching instruments because they re-enact thought experiments, allowing students to think deeper about the quantum-mechanical principles involved. Interference, wave-particle duality and entanglement are among the most important predictions of quantum mechanics. They are abstract and counter-intuitive. More recent concepts that help illustrate these subtleties include quantum erasure and delayed choice. In this article we present an experiment for the undergraduate laboratory that involves all of these issues or concepts. The experiment entails only minor modifications to a well known setup for doing single-photon interference. In this article we present the experiment, its results and a theoretical description.

PACS numbers: 00.00, 20.00, 42.10

Keywords: Delayed-Choice, Quantum Mechanics, Interference , Undergraduate Laboratory Submitted to: *Eur. J. Phys.*

1. Introduction

Quantum mechanics, one of the most successful physical theories ever invented, has baffled researchers since its inception. At its essence is quantum superposition or interference. Richard Feynman called it "the only mystery" (of quantum mechanics) [1]. Exacerbating the dilemma of interference is the generalization that matter behaves as a wave, a subject of much discussion between Bohr and Einstein, and known as wave-particle duality. Can we see an object behave as a wave and a particle simultaneously? This idea has generated numerous theoretical and experimental investigations, with always a tricky answer, that we see either one or the other but not both, yet, we can switch from one to the other quite easily. To this Bohr attributed a principle

of complementarity, that wave and particle are two complementary manifestations [2]. Furthermore, researchers have invoked quantum erasing [3, 4], a situation that while illustrating the subtleties of quantum mechanics, it creates more debate due to its counterintuitive arguments. In quantum erasing the presence or absence of interference can be decided after the light has passed through the interference apparatus. The essence of the phenomenon is distinguishability of paths, or the availability of path information: if the paths are indistinguishable, then there is interference (*i.e.* the light exhibits wave-like behavior); whereas if the paths are distinguishable because the path information is available (*i.e.* the light exhibits particle-like behavior by taking a definite path), then there is no interference [1]. Quantum erasing is about making the path information available or not, regardless of when this occurs, even if it happens after the light passes through the interferometer. As it has become commonplace in debates about quantum physics, the reactions of disbelief are quieted by successful experimental verifications [5, 6, 7].

In 1935 Einstein, Podolski and Rosen proposed a thought experiment (now known as EPR) to underscore that quantum mechanics was incomplete [8]. After communications with Einstein, Schrödinger understood a deeper situation predicted by quantum mechanics known as entanglement [9]. Quantum entanglement refers to the situation where two physical systems are in a state that cannot be factored into the product of the state of the individual subparts. The two systems are intimately linked in such a way that a measurement on one can define the state of the other one, regardless of how far apart the systems are located, a situation that Einstein derided as "spooky action at a distance" [10]. Beyond its intrinsic interest, entanglement has been used to perform tests of nonlocality and realism, always confirming the predictions of quantum mechanics [11].

Adding to the list of mind-twisters is the concept of delayed choice proposed by Wheeler [12]. Entanglement and wave-particle duality are at the heart of this phenomenon. The entanglement can be between two particles, but can also be an entanglement that involves the apparatus [13]. When dealing with situations involving entanglement, the final answer is obtained when both entangled particles are duly measured. However, quantum mechanics does not specify when those measurements are made. Wheeler emphasized this by explaining that the full picture of what happened in an experiment, interference or not, wave or particle, can be decided by a measurement on one of the entangled particles, which can be delayed to appear to define the physical picture after it happened. Our tendency to imagine what is "reality" before we take measurements is what gets us into trouble. Wheeler emphasized this by saying "a phenomenon is not a phenomenon until it is an observed phenomenon" [14]. Recent variations of the delayed choice conundrum puts the notions of "wave" and "particle" themselves in question [15], and by investigating "intermediary phenomena" where the quantum object is in a superposition of being a wave and a particle [16, 17, 18], i.e., situations where the quantum system is not entirely wave or particle.

Bohr is attributed the quote "Anyone who is not shocked by quantum theory has

not understood it." Apocryphal or not, the quote conveys the sentiment. Profound and counter intuitive but yet correct, demonstrations of quantum interference and entanglement are indisputable and unambiguous. They are even part of today's undergraduate laboratory [19, 20, 21, 22]. Armed by technological advances that simplify equipment and reduce costs, such experiences have become modern additions to the advanced undergraduate laboratory. They are compelling because they are able to demonstrate via experiments fundamental aspects of quantum physics [23].

Delayed-choice demonstrations, ever more sophisticated, continue to this day (see Ref. [24] for a review). In this article we describe an undergraduate-level experiment that illustrates delayed choice by manipulating the time-energy entanglement between two photons. Recently Ashby *et al.* presented a demonstration of delayed choice in the undergraduate laboratory where entanglement in polarization was used to make a delayed choice that decides whether the experiment records interference or not [25]. In our experiment we manipulate the entanglement in energy. Both types of experiments involve the generation of photons in an entangled state. One photon goes through an interferometer while the entangled partner travels a long distance after which it passes through a state-projection filter. The delayed character of the projection or measurement resulting from the passage through the filter is that it occurs after the other photon (the one going through the interferometer) has been detected. In the case of Ref. [25] quantum erasing was performed via polarization projections that change the quantum state to make the path information available or not [26, 27, 28]. In the experiment presented here the projection is done by an energy filter (a narrow bandpass optical filter), as described previously [21, 29]. Both experiments fall into the category of quantum erasers because the action that decides the experimental outcome occurs after the light has gone through the interference apparatus. We added the delayed-choice aspect of the experiment by inclusion of an optical delay so that the projection occurs after the partner photon (the one going through the interferometer) has been detected and no longer exists. The delayed-choice component is a relatively minor addition to a setup that is commonly used in undergraduate-lab experiments [21]. The issues that it raises make it compelling to implement in the undergraduate laboratory.

In section 2 we present a discussion of the experiment and the apparatus. We follow with the results in Sec. 3. We present two approaches to the explanation of the experiment in Sec. 4. In a first one we give a simplified version that is suitable for teaching purposes. A second one accounts for down-conversion in a more rigorous way. In Sec. 5 we present a comparison between a larger set of experimental results and the rigorous theory. Concluding remarks follow in Sec. 6. We have implemented this experiment in the context of a table-top lab for a course on quantum mechanics, so in a first Appendix (Sec. 7) we present a discussion of the experiment within the context of an undergraduate laboratory experience. The more technical aspects of the rigorous theory are presented in a second Appendix (Sec. 8).

2. The Experiment

In this article we present an experiment that uses two photons, created simultaneously, where one photon goes through an interferometer and the partner is send directly to a detector. The interferometer is of the Mach-Zehnder type, featuring two separate arms in a rectangular arrangement. The coincident arrival of the signals from the detection of the two photons is recorded. As the difference in path-length between the two arms of the interferometer is changed, so are the conditions for the interference. This type of experiment has become a classical demonstration of some of the puzzling aspects of superposition, that a quantum particle can interfere with itself. An important feature of this experiment is the energy entanglement between the two photons. The outcome of the experiment reveals that the interference of a single photon going through the interferometer also depends on its entangled partner and how both are detected.

We used the simplest type of photon-pair generation: type-I spontaneous parametric down-conversion (SPDC). Light from a blue-diode laser (nominally at 405 nm, but 402.8 nm in our case, with ∼50 mW of power output) was incident on a single beta-barium-borate (BBO) crystal (5-mm×5-mm×3-mm in size), producing pairs of down-converted photons. We selected the pairs with nearly the same energy (around a wavelength of 805.6 nm) to exit the crystal at ±3°. Photons were collected by multimode fibers that sent the light to single-photon avalanche photodiode detectors (Excelitas SPCM-EDU CD3375). These types of experiments have been described in detail previously [30, 31].

A schematic of the apparatus that we used is shown in Fig. 1. One of the mirrors of the interferometer was mounted on a translation stage that had a piezo-electric element as a spacer. The micrometer of the stage was used for coarse translations of the mirror (about 5-10 μm per "nudge" of the micrometer screw), but the piezo-electric component was used for changing the path in small increments (about 25 nm per step). By applying a voltage to the piezo-electric, its length was increased, pushing the translation stage and consequently the mirror, thereby changing the length of one of the paths. This was done sequentially by computer control producing a scan over a range of about 4 μm. This change was small enough to not affect the alignment. In an experiment of this type, as presented before [30], the outcome involves the observation of interference maxima and minima as the path-length difference of the interferometer is varied, revealing that when the two paths of the interferometer are indistinguishable, a single photon interferes with itself [21, 29, 32].

The photons created by parametric down-conversion conserve energy and momentum. If the energy of the incident photon is E_0, then the energies of the down-converted photons are E and $E_0 - E$. They leave the crystal in a narrow range of angles. The collection of these photons is done through small lens collimators that channel the light reaching them forming a small solid angle. For example, the calculated angular difference between 830 nm and 790 nm is 7.2 arc minutes. This corresponds to 2.1 mm at 1-m from the crystal. Within this solid angle the photons are indistinguishable by

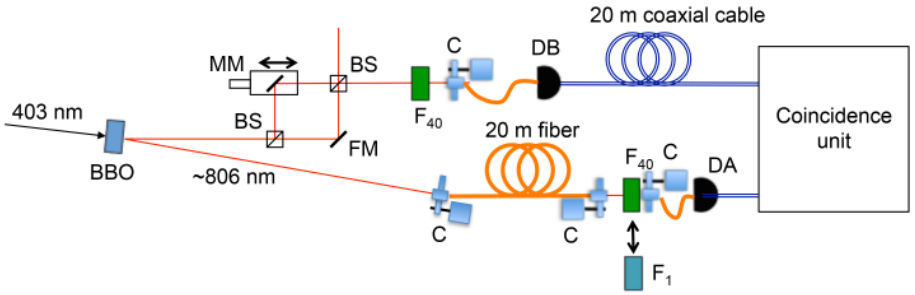

Figure 1. Schematic of the apparatus used. Optical elements include SPDC crystal (BBO), non-polarizing beam splitters (BS), fixed mirror FM, movable mirror on a translation stage (MM), fiber collimator (C), bandpass filters (F_{40} = 40 nm; F_1 = 1 nm), avalanche photodiode detectors (DA and DB).

their energy, and so they are in the non-separable state of superposition:

$$|\psi\rangle = \int C_0(\omega)|\omega\rangle_1|\omega_0 - \omega\rangle_2 d\omega, \tag{1}$$

where $C_0(\omega)$ is the amplitude of producing a given pair of energies $(E, E_0 - E)$, which we express more conveniently in terms of the angular frequency: $(\omega, \omega_0 - \omega)$, and where $\omega_0 = E_0/\hbar$ is the angular frequency of the pump beam. Thus, the above photons are entangled in energy, because their state cannot be separated into a product of the state of the individual photons. This type of entanglement is inherent to down-conversion. This entanglement in energy has been well recognized previously [29, 33], and has been used to perform violations of Bell inequalities in time and energy [34, 35, 36]. The time entanglement arises by the indistinguishability in the time at which the photons were created. This is analogous to the landmark thought experiment of EPR, where the entanglement in position and momentum is instead described in terms of time and energy by applying $k \to \omega/c$ and $x \to ct$ [36].

A key part of the apparatus was photon collection and detection. A bandpass filter was placed in front of the fiber collimators so that the bandwidth of the collected photons was restricted even further. (This is standard in these types of experiments.) This way, photon 1 went through the interferometer, passed through a bandpass filter (F_{40} of bandwidth 40 nm) and a 2-m optical fiber before reaching the single-photon detector (DB). To implement the delayed-choice aspect of the experiment we made special additions to previous versions of the single-photon interference experiment [30]. Photon 2 traveled in free space straight to a fiber collimator lens connected to an optical fiber. Normally this fiber would send the photons to a detector, similarly to photon 1, but in this case we used two consecutive fibers before sending photon 2 to its detector (DA). The first fiber was 20 m long, and was used as an optical delay. After this fiber, the photon was relaunched into free space, to then pass through a band-pass filter, a critical component of the experiment. Thereafter it was incident on a collimator to enter a 2-m fiber to finally reach the detector. This can be seen in the diagram of Fig. 1.

The optical delay imposed on photon 2 made it pass through the band-pass filter

about 90 ns after photon 1 was detected. We selected the length of fiber so that the filtering action was made clearly after the detection of photon 1 was in form of an electronic pulse. To record the partner photons we used an electronic coincidence unit (Altera DE2). Because the electronic pulse from the detection of photon 2 was delayed by the long optical fiber, we compensated it by adding a delay to the electronic signal from the detection of photon 1. This was implemented via a 20-m coaxial cable (type RG-58) to the path of the digital signal from detector DB, as shown in Fig. 1. Because the propagation speed of the electronic pulse through the cable is conveniently about 2/3 the speed of light, about the same as the propagation of the light through the 20-m fiber, we used the same length of extra electric cable for temporal compensation. We verified that without the cable there were no photon coincidence detections beyond the ones that occur due to the random arrival of non-partner photons (*i.e.*, the "accidental" coincidences). Photons arriving to the electronic unit within a time window of 40 ns were considered a coincidence.

The interference experiments involved changing the difference in path length of the two arms by amounts ΔL. Because knowing this value is an important aspect of the experiments, we discuss next how we measured it. We did this by recording the spectrum of the light from a small incandescent light bulb after it passed through the interferometer, a technique based on the Alford-Gold effect [37], which consists of the observation of fringes in the spectrum of broad-band light after passing through an interferometer. We placed the bulb before the first beam splitter of the interferometer, and placed an optical fiber after the second beam splitter of the interferometer. The fiber channeled the light to a spectrometer (Ocean Optics 2500). The difference in path produced a modulated spectrum, showing maxima and minima of interference. A maximum of wavelength λ_1 corresponds to an integer multiple of wavelengths, or

$$\Delta L = m\lambda_1, \tag{2}$$

where m is an integer. The adjacent maximum of longer wavelength λ_2 involves one less multiple of the wavelength, or

$$\Delta L = (m-1)\lambda_2. \tag{3}$$

Combining Eqs. 2 and 3, we get

$$m = \frac{\lambda_2}{\lambda_2 - \lambda_1}. \tag{4}$$

yielding

$$\Delta L = \frac{\lambda_1 \lambda_2}{\lambda_2 - \lambda_1}. \tag{5}$$

We measured the wavelength separations between adjacent maxima to obtain ΔL.

3. Results

In our experiments the difference in path lengths had a coarse value specified by ΔL. For each setting of ΔL we scanned the path difference further using the piezo-electric.

This way we could see the degree of interference in the measured pattern. We started the experiments with bandpass filters F_{40} on both photons, and with $\Delta L \sim 0$. We verified this by adjusting ΔL such that the *entire* spectrum was undergoing a maximum or minimum of interference; the equivalent to observing "white-light fringes." We then proceeded to increase ΔL in increments of tens of micrometers, until the interference disappeared. For each setting of ΔL we took a white-light spectrum for determining the value of ΔL, as described above.

A representative summary of our data is shown in Fig. 2. In panes (a), (d), (g) and (j) we show the interference patterns taken by scanning a piezoelectric element in the interferometer. We plot the data with uncertainties $\sqrt{N}$, although in all cases these are about the size of the symbols. We fit the data with the function

$$f(v) = N_0[1 + V\cos(b_0 + b_1 v + b_2 v^2 + b_3 v^3)], \tag{6}$$

where the fitting parameters are N_0, V, b_i, and where v is the voltage applied by the piezo-electric element. We did a non-linear fit of the phase because of the well-known nonlinearity in the piezo-electric. The fitted visibilities are displayed in the upper-right of the graphs. In panes (b), (e), (h) and (k) we show the white-light spectra, with the path-length difference at $v = 0$ obtained by the spectrum fringes.

For the data of Fig. 2, both photons go through the same filters F_{40}. Because the degenerate wavelength (805.6 nm) was not centered on the filter pass-band (800 nm), the effective bandwidth was $\delta\lambda \sim 27$ nm. The visibility of the interference pattern was determined by the coherence length of the light, given by [38]

$$\ell_c = \frac{\lambda^2}{\delta\lambda}. \tag{7}$$

The light forms an energy wavepacket with a temporal width $\tau_c \sim \ell_c/c$, also known as the coherence time. For our experimental parameters the effective coherence time corresponds to $\tau_c = 80$ fs (or equivalently, $\ell_c = 24$ μm). As ΔL was increased, the amplitude wavepackets of the photon traveling through the two arms of the interferometer became temporally displaced by $t = \Delta L/c$. This provided an element of temporal distinguishability for the paths: a which-way marker [39, 40]. As a consequence, the visibility of the interference pattern decreased, as seen in Fig. 2. To have a qualitative picture of the overlap of the amplitudes, in panes (c), (f), (i) and (l) we show a calculation of Gaussian functions of full-width at half maximum of τ_c separated by the time difference t, mimicking the envelope of the wavepacket.

The data set of Fig. 2 can also be viewed as a transition from wave-like behavior when $t < \tau_c$, to the particle-like behavior when $t > \tau_c$. For each case correspond an "intermediary phenomenon" between wave ($\Delta L \sim 0$) and particle ($\Delta L \sim 81$ μm), as described above. Interference disappears because the paths become distinguishable in time. An arrival-time measurement can in principle reveal unambiguously the path taken by the light (i.e., the photon arriving earlier denoting the photon taking the short path, and the converse). In this case, the which-way marker is t.

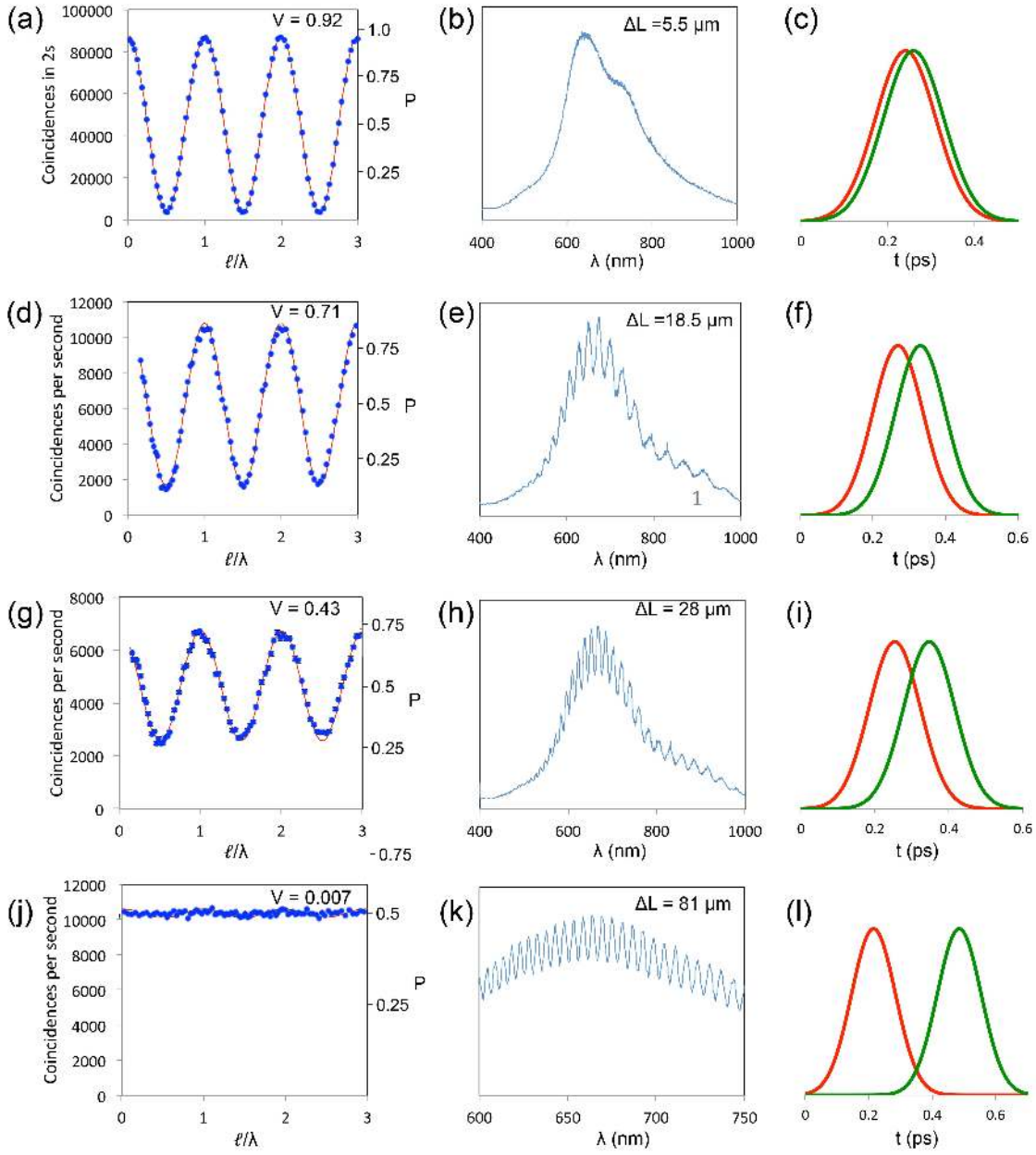

Figure 2. Graphs of the interference pattern (a,d,g,j), corresponding white-light spectra (b,e,h,k) and simulated Gaussian wave packet separation for different path-length difference of the interferometer ΔL, shown as inserts (uncertainties were of the order of 5%). Panes (a,b,c), (d,e,f), (g,h,i), (j,k,l) are sets with the same experimental parameters. Symbols are measured data with values given by the left side of the graphs. The solid line is the least squares fit to the data, with the right-side scale giving the probability obtained from the fits.

A change in the bandwidth of the filter would alter the conditions of the interference. The above picture works as long as the two photons are identical, so the physics of the phenomenon is focused on the photon going through the interferometer. However, we can exploit the energy entanglement of the light and change the bandwidth of the filter

of photon 2, which is not going through the interferometer [21, 29]. Because coincidences are recorded, this effectively changes the bandwidth of light showing the interference. We then applied Wheeler's delayed-choice argument: the passage of photon 2 through the filter occurred well after photon 1 had been detected, introducing an apparent causal contradiction. However, this is consistent with the predictions of quantum mechanics, as discussed below.

In Fig. 3(a) we show the pattern obtained after replacing the filter on photon 2 with one with a bandwidth of 1 nm (F_1). This was taken after the scan of Fig. 2(j), which corresponds to $\Delta L = 81$ μm. Decreasing the bandwidth made the effective coherence time about 27 times larger: $\tau_c \sim 2.1$ ps (or equivalently $\ell_c \sim 640$ μm). We display the equivalent change in the width of the photon wavepacket pictorially in Fig. 3(b). It can be seen that the new bandwidth reveals much overlap. So much that the paths become mostly temporally indistinguishable. Thus, we can say that the path information was erased, as manifested by the reappearance of interference fringes seen in Fig. 3(a). Because the narrower filter restricted the number of recorded photons, the coincidence rate decreased by about a factor of 16. We note that the wavepackets that we depict are two-photon wavepackets.

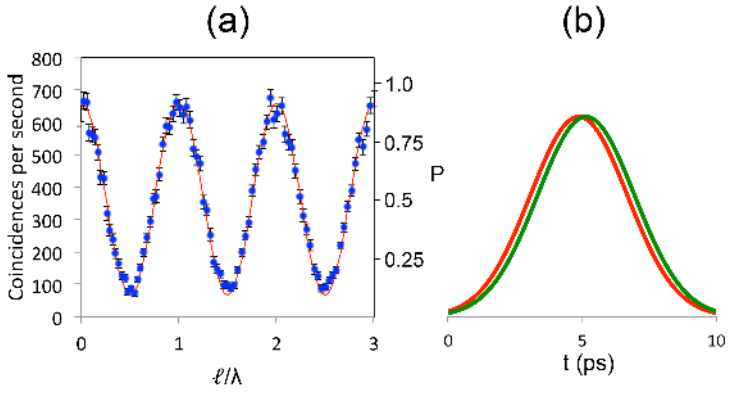

Figure 3. Graph of (a) the interference pattern, and (b) the simulated Gaussian wave packet envelope separation for a path-length difference of the interferometer of $\Delta L = 81$ μm but with photon 2 going through filter F_1. The data are represented by symbols and values are given by the scale on the left side of the graphs, with the right-side scale giving the probability obtained from the fits. The solid line is the least-squared fit to the data with The fitted visibility was $V = 0.76 \pm 0.05$.

4. Theory

The experiment described above presents a picture that at first appears troubling. How can a measurement determine the degree of interference after the light going through the interferometer has been detected? The problem with this argument is that we are assigning a reality to a situation where quantum mechanics does not specify a definite

reality. From the quantum mechanics perspective there is no problem: the reality can be undefined. This situation brings relevance to Wheeler's statement cited earlier regarding the observation of a phenomenon. Our classical intuition leads us to assign a reality to a phenomenon before it is completely measured. We are going to describe the theoretical explanation at two levels: a semiquantitative one, and another one that accounts the source of photons in a more rigorous way.

4.1. A Simple Model

We begin with the wavefunction of Eq. 1. Photon 1 goes through the interferometer. Let us assume that there are no losses, so the interferometer can be represented by the unitary operator $\hat{U}$ acting on photon 1. The coefficients of reflection and transmission of the beam splitters are $i/\sqrt{2}$ and $1/\sqrt{2}$, respectively. The path-length difference of the arms of the interferometer ΔL results in a difference in arrival time t of the light taking the two paths of the interferometer. After the interferometer the state of the photons is to within an overall phase, and as of yet unnormalized, given by

$$|\psi'\rangle = \hat{U}|\psi\rangle = \frac{1}{2}\int C_0(\omega)(1+e^{\mathrm{i}\omega t})|\omega\rangle_1|\omega_0-\omega\rangle_2 d\omega. \tag{8}$$

After the interferometer photon 1 goes through the bandpass filter with transmission function $C_1(\omega)$. Photon 2 has a longer trip through the 20-m fiber, after which it reaches the bandpass filter with transmission function $C_2(\omega)$. Detectors following the filters complete the energy-projection measurement into states

$$|\psi'\rangle_i = \int C_i(\omega')|\omega'\rangle_i d\omega' \tag{9}$$

$i = 1, 2$. Thus, passage through the two filters projects the state as

$$|\psi''\rangle = \int C_1(\omega')|\omega'\rangle_1\langle\omega'|_1 d\omega' \int d\omega'' C_2(\omega'')|\omega''\rangle_2\langle\omega''|_2 \int d\omega C_0(\omega)\hat{U}|\omega\rangle_1|\omega_0-\omega\rangle_2. \tag{10}$$

Orthogonality of the energy eigenstates is expressed as

$$\langle\omega'|\omega\rangle_1 = \delta(\omega'-\omega) \tag{11}$$

and

$$\langle\omega''|\omega_0-\omega\rangle_2 = \delta(\omega''-\omega_0+\omega), \tag{12}$$

which leaves the unnormalized state of the light as

$$|\psi''\rangle = \int d\omega\ C(\omega)\hat{U}|\omega\rangle_1|\omega_0-\omega\rangle_2. \tag{13}$$

where

$$C(\omega) = C_0(\omega)C_1(\omega)C_2(\omega_0-\omega). \tag{14}$$

The frequency (or energy) eigenstates used above are similar to the position and momentum eigenstates used by wave mechanics in problems such as the particle in a box. They constitute a convenient continuous basis, but they do not imply that the photons are in an energy eigenstate of infinitesimal width [41, 42]. Analogous to

looking for the probability of finding the particle in a region of the space within the box, we measure the energy of the photons by the filtering action, which involves a frequency/energy measurement over a finite bandwidth.

The final probability then becomes

$$P = \frac{1}{4}\int |C(\omega)|^2 \left|(1+e^{\mathrm{i}\omega t})\right|^2 d\omega, \tag{15}$$

$$= \frac{1}{2}\int |C(\omega)|^2 \left[1+\cos(\omega t)\right] d\omega, \tag{16}$$

The relevant part of Eq. 16 is indeed the energy function $C(\omega)$, which determines whether the integral becomes a harmonic variation with the time difference t, or a constant due to a wide range of energies involved. However, this probability is independent of when the measurements are performed. The order of the measurements is immaterial because they apply to the distinct energy subspaces of the two photons.

Let us illustrate the answer for a simple case to understand the two extremes of this problem. Suppose $C(\omega)$ is given by:

$$|C(\omega)|^2 = \begin{cases} 1/(\omega_2-\omega_1) & \omega_1 \le \omega \le \omega_2 \\ 0 & \text{otherwise} \end{cases} \tag{17}$$

This is a flat-top bandwidth. In this case the integral is straightforward to solve giving

$$P = \frac{1}{2}\left(1+\frac{\sin\alpha}{\alpha}\cos\overline{\omega}t\right), \tag{18}$$

where $\alpha = \Delta\omega t/2$, with $\Delta\omega = \omega_2-\omega_1$, and $\overline{\omega} = (\omega_1+\omega_2)/2$. Note also that

$$\alpha = \frac{\pi t}{\tau_c} = \frac{\pi\Delta L}{\ell_c}. \tag{19}$$

Thus, when $t \ll \tau_c$ (or equivalently $\Delta L \ll \ell_c$) we have $\sin\alpha/\alpha \to 1$, so the probability is

$$P = \frac{1}{2}\left(1+\cos\overline{\omega}t\right), \tag{20}$$

which corresponds to interference that varies with the time difference t. As ΔL increases to the limit when $\Delta L \gg \ell_c$, results in $\alpha \to \infty$ or $\sin\alpha/\alpha \to 0$; the interference disappears and the probability becomes

$$P = 1/2. \tag{21}$$

4.2. A More Rigorous Theory Incorporating the Down-Converted Photon Source in the Experiment

4.2.1. Overview The previous discussion gives the quantum probabilities for "wave" (Eq. 20) or "particle" (Eq. 21), which can be associated to Fig. 2a and Fig. 2j respectively. After normalization, they depend on the relation between ℓ_c and ΔL. However, this can be improved in order to predict the other intermediate observed probabilities Fig. 2d and Fig. 2g and predict also the visibility of all patterns (included the one found after erasure, Fig. 3a).

First, we summarize the main concepts and definitions related to the interference, filtering and counting of the *biphoton* or entangled pair of photons we used in the experiment; then we find the quantum probabilities as a function of both the spectral bandwidth of the filters (related to ℓ_c) and the optical path difference in the interferometer ΔL. As a consequence, these probabilities are modulated by a Gaussian-like amplitude. This modulation is precisely the visibility observed in the patterns. The mathematical prerequisites of this new model, although a little bit more sophisticated, follow the same conceptual steps as the previous one. It is suitable for an introductory quantum optics course.

4.2.2. Counting Rate, Joint Spectral Amplitude and Biphoton State The patterns in Fig. 2 relate coincidence counts with smooth displacements in the path difference of the arms of the interferometer. In quantum optics, these coincidence counts R_c are proportional to the second-order correlation function $G^{(2)}$ through [43]:

$$\begin{aligned} R_c &\propto \int_T dt_1 dt_2 G^{(2)}(\vec{r}_1, t_1; \vec{r}_2, t_2) \\ &= \int_T dt_1 dt_2 |\langle 0|\hat{E}_2^{(+)}\hat{E}_1^{(+)}|\psi\rangle|^2. \end{aligned} \tag{22}$$

Where $G^{(2)}$ carries the information of where and when the coincidence takes place. More specifically, it is about the coincidence of fields arriving to the detectors. $E_\mu^{(+)}$ accounts for the field operators at the positions $(\vec{r}_\mu, t_\mu)$ of the detector μ ($\mu = 1, 2$). As in the simple model, "1" and "2" are the indices labeling the photons. $E_1^{(+)}$ represents the field operator for the detector outside the interferometer, whereas $E_2^{(+)}$ is the operator for the detection of the photon that does not go trough the interferometer. They are given by

$$\hat{E}_1^{(+)}(t_T, t_R) = \bar{t}_1\bar{r}_2 \int d\omega_1 \hat{a}(\omega_1) e^{-\mathrm{i}\omega_1 t_T} + \bar{r}_1\bar{t}_2 \int d\omega_1 \hat{a}(\omega_1) e^{-\mathrm{i}\omega_1 t_R}, \tag{23}$$

and

$$\hat{E}_2^{(+)}(t_2) = \int d\omega_2 \hat{a}(\omega_2) e^{-\mathrm{i}\omega_2 t_2}, \tag{24}$$

where $\bar{t}_\mu$ and $\bar{r}_\mu$ represent the transmission and reflection amplitudes for each beam splitter, and t_T is the time of flight through the transmission branch and t_R is the time of flight through the reflection branch. $\hat{a}(\omega_\mu)$ are the annihilation operators for photon μ.

In the expressions above we account for the detection aspect. On the production side, the joint spectral amplitude (JSA) for the pairs of photons produced in the Type-I-SPDC process can be described in a general way using the expression [44]:

$$\Phi(\Omega_1, \Omega_2) = \mathcal{N} \exp\left[-\frac{(\Omega_1 - \Omega_2)^2}{4\sigma_-^2} - \frac{(\Omega_1 + \Omega_2)^2}{4\sigma_+^2} \right], \tag{25}$$

where $\Omega_\mu = \omega_\mu - \omega_\mu^0$, is the detuning for each photon μ ($\mu = 1, 2$), $\mathcal{N}$ is a normalization factor, and σ_+ and σ_- depend on the experimental details of the SPDC process [45].

In the experiment we are considering Gaussian-interference filters in front of the detectors. To model such filters, we are going to introduce the functions $f_\mu(\Omega_\mu) \propto \exp\left[-\Omega_\mu^2/4\sigma_\mu^2\right]$ (these are the $C(\omega'_\mu)$ functions of the previous model). Thus, the filtered JSA takes the form

$$\tilde{\Phi}(\Omega_1,\Omega_2) = \mathcal{N} f_1(\Omega_1) f_2(\Omega_2) \exp\left[-\frac{(\Omega_1-\Omega_2)^2}{4\sigma_-^2} - \frac{(\Omega_1+\Omega_2)^2}{4\sigma_+^2}\right]. \tag{26}$$

With this, a more complete representation the state of the biphoton in Eq. 1 after the filters is

$$|\psi\rangle_{\text{SDPC}} = \int d\omega_1 d\omega_2 \tilde{\Phi}(\omega_2,\omega_1)\hat{a}_2^\dagger(\omega_2)\hat{a}_1^\dagger(\omega_1)|0\rangle. \tag{27}$$

Here, $\hat{a}^\dagger(\omega)$ are the *creation operators* of photons 1 and 2 acting on the vacuum state $|0\rangle$. The final step involves putting the production and detection parts together into Eq. 22. The end result for the coincidence detection probability is:

$$P = \frac{1}{2}(1 + V\cos\omega_1^0 t), \tag{28}$$

where the visibility V depends on experimental bandwidths and on the path length difference. It is given by

$$V = \exp\left[-\frac{\gamma\, t^2}{4(\alpha\gamma-\beta^2)}\right], \tag{29}$$

and where α, β and γ depend on the bandwidth of the filters, the wavelength of the photons, and the bandwidth of the pump photons in the SPDC process. As mentioned at the beginning of this section, Eq. 28 not only reproduces the results already obtained by the qualitative model, i.e., the "wave" behavior (with V=1, which gives Eq. 20) and the "particle" behavior (with V=0, which gives Eq. 21); but also the intermediate phenomena, such as $V = 0.71$ in Fig. 2d, $V = 0.43$ in Fig. 2g and $V = 0.76$ in Fig. 3a, with the latter corresponding to the recovered interference after the delayed-choice erasure. Importantly, we stress that the visibility of the interference of photon 1 is now a function of ℓ_c and ΔL. The details of how V is obtained are presented in Sec. 8.

5. Comparison of Experiment with Theory

Figure 4 shows a graph summary of all of the measurements. We took data with the 40-nm filters by increasing ΔL up to about 81 μm, as described earlier. As this was done, the measured visibility decreased gradually to zero, as seen in the figure. A first data set (diamonds) was taken without delayed choice (i.e., without optical and electronic delays). At $\Delta L = 81$ μm we changed the filter on photon 2 to 1-nm bandwidth and the interference reappeared (large circle, corresponding to an average of 4 measurements), as shown by a dramatic jump in the visibility. We also took data by placing the 1-nm filter on the photon that traveled through the interferometer, and observed the same result. The conclusion is that it does not matter where we put the 1-nm filter. This is because the recorded interference is that of a two-photon state.

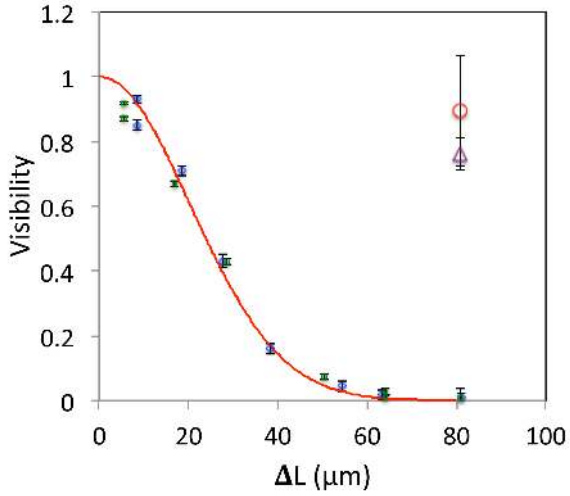

Figure 4. Graph of the visibility. Small symbols (blue diamonds and green circles) correspond to data taken with both filters of the same bandwidth. The large round red circle corresponds to the narrow filter placed on the photon not going through the interferometer. The large purple triangle corresponds to placing the filter after the optical delay in the path of the photon not going through the interferometer. Solid line is the calculation of the visibility by the rigorous theory.

We then switched to the delayed-choice situation (i.e., adding the optical and electric delays), mentioned above, and measured similarly high visibility (the triangle in Fig. 4). Subsequently we put back the broad filters and reduced ΔL keeping the delayed choice components in place. This is shown in the second set of data in the figure (small triangles). These data are also consistent with the data taken as ΔL was increased with no delayed choice. Finally, we have repeated the experiment several times in different order and with different configurations (including one where photons traveled in opposite directions while on free space), and obtained similar results. These included several instances where students did the experiment (including setup and alignment) as part of teaching laboratories in 2018 and 2019.

The solid line shown in the graph is the visibility function V of Eq. 29 by using $t = \Delta L/c$ when both photons 1 and 2 were filtered with F_{40}. As can be seen, the model is in excellent quantitative agreement with the measurements. Figure 5 shows the dependence of the calculated V with the bandwidth of the filter on photon 2 (solid line), when ΔL was fixed at 81μm. The theory for V takes into account the effective bandwidth due to the difference between the filters' center wavelength and the degenerate wavelength of the down-converted photons. This is the configuration when erasure takes place. We show the data with the two corresponding filters.

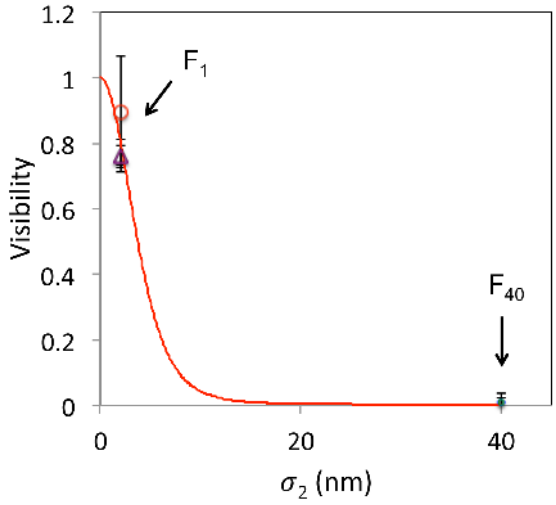

Figure 5. Visibility as a function of the bandwidth σ_2 of the filter on photon 2 before and after erasure, using F_{40} and F_1, respectively, for fixed $\Delta L = 81\mu$m. The solid line is the visibility given by Eq. 29, whereas the symbols are the experimental measurements corresponding to the two filters used.

6. Discussion and Conclusions

From the results presented above we are left with the conclusion that the interference pattern in this experiment cannot solely be attributed to a single photon. It is the interference of two photons, even though only one photon goes through the interferometer. Even if we are convinced of the notion of entanglement, and that "spooky action at a distance" indeed occurs we face another dilemma: what spooky action is there if the photon affected by it no longer exists? What does the projection on second photon do? It would not make sense to think that the action on one photon can affect the other into the past. The resolution is quite typically quantum-mechanically agnostic. The signal from first photon going through the interferometer and the wide-bandwidth filter is recorded. The wave-particle information is stored in the temporal dependence of the data. That is already a projection of the initial state of the light produced by the source. The measurement on the second photon going through the filter of variable bandwidth provides a temporal filtering action of the events when both photons are detected. The choice of filter selects from the data that is already present electronically, and thus determines the degree of interference or wave-particle character that is seen in the jointly measured data. The theoretical description from above tells us that the way to understand quantum mechanics is to avoid visualizing situations that have not been defined by measurements, and following Wheeler, accepting that a phenomenon is not such until it is measured.

In conclusion, we present an addition to the undergraduate experiments on the interference of photons produced by parametric down-conversion to involve quantum

erasure and delayed choice. These features are possible due to the energy entanglement that is present in down-conversion. The selection of filters on a delayed detection of a photon can determine whether one sees interference or not after the entangled partner photon has passed through an interferometer and been detected. It is an experiment that illustrates the challenging concepts of quantum erasure and delayed choice. The experiments are undoubtedly striking. Our intuition is classical, so we have to work hard at learning how to interpret quantum nature despite of our intuitive tendencies. Perhaps that is what makes the experiments powerful in teaching, because they falsify misconceptions. We can be dissuaded by theory or simulation, but there is nothing more convincing and tangible than nature itself.

Acknowledgments

We thank B. Khajavi and J.A. Jones for help useful discussions and C.H. Holbrow for valuable feedback. This work was funded by NSF grant PHY-1506321.

References

[1] Feynman R P, Leighton R B and Sands M, *The Feynman Lectures on Physics* (Addison-Wesley, Reading, 1965) V. 3.

[2] Bohr, N, 1928 The quantum postulate and the recent development of atomic theory *Nature* **121** 580

[3] Scully M O and Drühl K 1982 Quantum eraser: A proposed photon correlation experiment concerning observation and 'delayed choice' in quantum mechanics *Phys. Rev. A* **25**, 2208

[4] Scully M O, Englert B-G and Walther H 1991 Quantum optical tests of complementarity *Nature* **351** 111

[5] Zou X Y, Wang L J and Mandel L 1991 Induced Coherence and Indistinguishability in Optical Interference *Phys. Rev. Lett.* **67**, 318

[6] Kwiat P G, Steinberg A M and Chiao R Y 1992 Observation of a 'quantum eraser': A revival of coherence in a two-photon interference experiment *Rev. A* **45**, 7729

[7] Kim Y-H, Yu R, Kulik S P, Shih Y and Scully M O 2000 Delayed 'choice' quantum eraser *Phys. Rev. Lett.* **84**, 1

[8] Einstein A, Podolsky B and Rosen N 1935 Can quantum-mechanical description of physical reality be considered complete? *Phys. Rev.* **47** 777

[9] Schrödinger E (1935) The present situation in quantum mechanics *Proc. Am. Philosoph. Soc.* **124** 323

[10] Born M 2005 *The Born-Einstein Letters 1916-1955 Friendship, Politics and Physics in Uncertain Times* (Macmillan, Houndmills, Basingstoke, Hampshire, New York)

[11] Aspect A 2015 Closing the door on Einstein and Bohr's quantum debate *Physics* **8** 123

[12] Wheeler J A 1983 Law without law in *Quantum Theory and Measurement* ed J A Wheeler and W H Zurek (Princeton NJ: Princeton University Press) p 182

[13] Englert B-G, Scully M O and Walther H 1999 Quantum erasure in double-slit interferometers with which-way detectors *Am. J. Phys.* **67** 325

[14] Miller W A and Wheeler J A 1983 Delayed-choice experiments and Bohr's elementary quantum phenomenon *Proc. Int. Symp. Foundations of Quantum Mechanics* p 140

[15] Jacques V, Wu E, Grosshans F, Treussart F, Grangier P, Aspect A and Roch J-F Delayed-choice test of quantum complementarity with interfering single photons Phys. Rev. Lett. **100** 220402

[16] Ionicioiu R and Terno D R 2011 Proposal for a Quantum Delayed-Choice Experiment *Phys. Rev. Lett.* **107**, 230406
[17] Tang J-S, Li Y-L, Xiang G-Y and Guo G-C 2012 Realization of quantum Wheeler's delayed-choice experiment *Nat. Photon.* **6**, 600
[18] Auccaise R, Serra R M, Filgueiras J G, Sarthour R S, Oliveira I S and Cleri L C, 2012 Experimental analysis of the quantum complementarity principle *Phys. Rev. A* **85**, 032121
[19] Dehlinger D and Mitchell M W 2002 Entangled photons, nonlocality, and Bell inequalities in the undergraduate laboratory *Am. J. Phys.* **70**, 903
[20] Thorn J J, Neel M S, Donato V W, Bergreen G S, Davies R E and Beck M 2004 Observing the quantum behavior of light in an undergraduate laboratory *Am. J. Phys.* **72**, 1210
[21] Galvez E J, Holbrow C H, Pysher M J, Martin J W, Courtemanche N, Heilig L and Spencer J 2005 Interference with correlated photons: Five quantum mechanics experiments for undergraduates *Am. J. Phys.* **73**, 127
[22] Lukishova S G 2017, Quantum optics and nano-optics teaching laboratory for the undergraduate curriculum: teaching quantum mechanics and nano-physics with photon counting instrumentation *Proc. SPIE* **10452** 104522I
[23] Galvez E J 2014 Resource Letter SPE-1: Single-Photon Experiments in the Undergraduate Laboratory *Am. J. Phys.* **82** 1018
[24] Ma X-S, Kofler J and Zeilinger A 2016 Delayed-choice gedanken experiments and their realizations *Rev. Mod. Phys.* **88**, 015005
[25] Ashby J M, Schwarz P D and Schlosshauer M 2016 Delayed-choice quantum eraser for the undergraduate laboratory *Am. J. Phys.* **84** 95
[26] Walborn S P, Terra Cunha M O, Padua S, and Monken C H 2002 Double-slit quantum eraser *Phys. Rev. A* **65** 033818
[27] Gogo A, Snyder W D and Beck M 2005 Comparing quantum and classical correlations in a quantum eraser *Phys. Rev. A* **71**, 052103
[28] Pysher M J, Galvez E J, Misra K, Wilson K R, Melius B C and Malik M 2005 Nonlocal labeling of paths in a single-photon interferometer, *Phys. Rev. A* **72**, 052327
[29] Kwiat P G and Chiao R Y 1991 Observation of a nonclassical Berry's phase for the photon, *Phys. Rev. Lett.* **66**, 588
[30] Galvez E J 2010 Qubit quantum mechanics with correlated-photon experiments *Am. J. Phys.* **78**, 511
[31] URL: http://departments.colgate.edu/physics/pql.htm
[32] Grangier P, Roger G and Aspect A 1986 Experimental evidence for a photon anticorrelation effect on a beam splitter: A new light on single-photon interferences *Europhys. Lett.* **1** 173
[33] Saldanha P and Monken C H 2013 Energy and momentum entanglement in parametric downconversion *Am. J. Phys.* **81**, 28
[34] Franson J D 1989 Bell inequality for position and time *Phys. Rev. Lett.* **62** 2205
[35] Brendel J, Mohler E, Martienssen W (1992) Experimental test of Bell's inequality for energy and time *Europhys. Lett.* **20**, 575
[36] Kwiat P G, Steinberg A M and Chiao R Y 1993 High visibility interference in a Bell-inequality experiment for energy and time *Phys. Rev. A* **47**, R2472
[37] Salazar-Serrano L J, Valencia A and Torres J P Observation of spectral interference for any path difference in an interferometer *Opt. Lett.* **39** 4478
[38] Born M and Wolf E 1999 *Principles of Optics* 7th edn (Cambridge: Cambridge University Press)
[39] Englert B-G 1999 Remarks on some basic issues in quantum mechanics *Z. Naturforsch.* **54a** 11
[40] Ferrari C and Braunecker B 2010 Entanglement, which-way measurements, and a quantum erasure *Am. J. Phys.* **78**, 792
[41] Ballentine L E 1998 *Quantum Mechanics: A Modern Development* (World Scientific Publishing Co.)
[42] Schwindt J-M 2016 *Conceptual Basis of Quantum Mechanics* (Springer International Publishing,

Switzerland)
[43] Shih Y 2003 Entangled biphoton source property and preparation *Rep. Prog. Phys.* **66**, 1009
[44] Zielnicki K, Garay-Palmett K, Cruz-Delgado D, Cruz-Ramirez H, O'Boyle M, Fang B, Lorenz V, U'Ren A and Kwiat P 2018 Joint spectral characterization of photon-pair sources *J. Mod. Optic.* **65**, 1141
[45] Valencia A, Ceré A, Shi X, Molina-Terriza G and Torres J P 2007 Shaping the Waveform of Entangled Photons *Phys. Rev. Lett.* **99**, 243601.

7. Appendix: Educational Implementation

The outcomes of these and other experiments can be used to reach a deeper understanding of quantum physics. We are fortunate that technology has advanced to the point that undergraduates can do these experiments and grapple with the same issues that the professors do. Thus, it is a learning experience, for both! As mentioned earlier, there is a set of entangled-photon experiments that can now be set up on an optical breadboard (as small as 2-ft×5-ft) using optical and hardware components that do not cost more than $1500 per item. At Colgate University we have a lab portion of an upper-level course on quantum mechanics. We have six experiments, and students set up and align each in the course of one or two weekly 3-4 hour sessions, and do the experiments in the following week. We instituted this method of alignment and experimentation in our offering in 2018. Details of these are available on our website [31]. Student feedback was overwhelmingly positive, as students appreciated building an apparatus from scratch and then making striking experimental verifications. That is, they did it all, with no laboratory magic performed by the professor or a sophisticated machine.

Regarding the delayed-choice experiment specifically, there are already several experiments described in earlier publications that involve single-photon interference with heralded photons [21, 30]. These experiments can easily and inexpensively be converted into delayed-choice experiments. The additional components are listed in Table 1. We added the least expensive commercial fiber spectrometer, which may already be in use for alignment of single-photon experiments, but which is a critical measurement device in these experiments. Very importantly, the additions do not make the experiment harder. They involve some alignments, but these are minor compared to the ones involved setting up the single-photon interference apparatus.

We wish to note one technical difficulty that we experienced in the course of the experiments. It involves the bandwidth of the filters. One could encounter these difficulties easily, so it is important to be aware of them. The most convenient choice of pump laser is the popular gallium-nitride blue diode laser. They are set to a nominal wavelength of 405 nm. One can obtain them at very low cost: from $20 laser pointers to current-control modules for about $300. However, the wavelength of these lasers can easily vary within a range of 10 nm. The nominal wavelength of down-converted photons is 810 nm, but then the variation in the source can signify a 20-nm variation. The bandpass filters that one can purchase off-the-shelf have a center wavelength that

Table 1. Components that are needed to expand a heralded photon experiment to delayed choice.

Component	Vendor	Model	Price (US$)
20-m multimode fiber	Thorlabs	Mater. Res. Express	286
20-m coaxial RG-58 cable	Mouser	115101-19-M20.0	51
1-nm filter centered at 810 nm	Andover	810.0/1.0-53343	345
Fiber collimator	Thorlabs	F220FCB	145
Mirror mount	Thorlabs	KM100T	64
Mounting accessories	Thorlabs	AD11F, SM1D12,MB175,TR3,RA90	148
Fiber Spectrometer	Vernier	VSP-EM	800

can be chosen to be either 800 nm or 810 nm. Thus, one can encounter a situation where the degenerate wavelength of the down-converted photons is outside the band-pass of the filters. If that is the case, in the experiment one will record photon counts at the other nearby wavelengths but no coincident detections, because one member of a pair is always blocked. We experienced such a situation before. In the case presented here, the degenerate wavelength was not centered about the bandpass of the filters, 40 nm. Thus only a fraction of the photons passing through the filters were partners. This realization and additional measurements led us to conclude that the effective bandwidth of the pairs (i.e., from Eq. 14) was 27 nm. Our recommendation is that users make measurements of the pump laser wavelength before purchasing the filters so that the appropriate ones are acquired. A measurement of filter transmission curves is in any case needed to determine the effective bandwidth. This is easily done by placing the filter in between a broadband source (e.q., incandescent bulb) and the spectrometer input. Alternatively, a more expensive laser option (between $6000 and $7000) allows one to specify the exact wavelength, in modules with greater stability and temperature control.

8. Appendix: Explicit Derivation of the Coincidence Counts

In order to obtain P in Eq. 28, we start by finding the wave function of the biphoton in the time integral Eq. 22. Considering the interferometer structure, we have that $\hat{E}_1^{(+)} = \hat{E}_T^{(+)} + \hat{E}_R^{(+)}$, and with this we have

$$\begin{aligned}\langle 0|\hat{E}_2^{(+)}\hat{E}_1^{(+)}|\psi\rangle &= \langle 0|\hat{E}_2^{(+)}\hat{E}_T^{(+)}|\psi\rangle + \langle 0|\hat{E}_2^{(+)}\hat{E}_R^{(+)}|\psi\rangle \\ &= \Psi_T(t_T, t_2) + \Psi_R(t_R, t_2),\end{aligned} \tag{30}$$

which in turn gives,

$$|\langle 0|\hat{E}_2^{(+)}\hat{E}_1^{(+)}|\psi\rangle|^2 = |\Psi_T|^2 + |\Psi_R|^2 + 2\Re(\Psi_T^*\Psi_R), \tag{31}$$

where the last term, $2\Re(\Psi_T^*\Psi_R)$ specifies the interference. The amplitude through the "T" path is

$$\Psi_T(t_1^T, t_2) = \langle 0| \left\{ \int d\omega_2' \hat{a}(\omega_2') e^{-\mathrm{i}\omega_2' t_2} \right\} \left\{ \frac{\mathrm{i}}{2} \int d\omega_1' \hat{a}(\omega_1') e^{-\mathrm{i}\omega_1' t_1^T} \right\} |\psi\rangle \tag{32}$$

$$= \frac{\mathrm{i}}{2}\int d\omega_1' d\omega_2' d\omega_1 d\omega_2 \tilde{\Phi}(\omega_1,\omega_2) e^{-\mathrm{i}\omega_2' t_2} e^{-\mathrm{i}\omega_1' t_1^T} \times \tag{33}$$

$$\times \langle 0|\hat{a}(\omega_2')\hat{a}(\omega_1')\hat{a}^\dagger(\omega_1)\hat{a}^\dagger(\omega_2)|0\rangle \tag{34}$$

$$= \frac{\mathrm{i}}{2} e^{-\mathrm{i}(\omega_2^0 t_2 + \omega_1^0 t_1^T)} \int d\Omega_1 d\Omega_2 e^{-\mathrm{i}\Omega_2 t_2} e^{-\mathrm{i}\Omega_1 t_1^T} \tilde{\Phi}(\Omega_1,\Omega_2), \tag{35}$$

where the simplification of the intermediate integral was done by using the commutation relation $[\hat{a}(\omega), \hat{a}^\dagger(\omega')] = \delta(\omega - \omega')$, and also by introducing the detuning variable $\Omega_\mu = \omega_\mu - \omega_\mu^0$, $\mu = 1, 2$, and factoring the constant terms. Another simplification can be done on the last integral by taking into account that t and Ω are conjugated variables. Indeed, this integral can be solved by the application of the double Fourier transform:

$$\Psi_T(t_1^T, t_2) = \frac{\mathrm{i}}{2} e^{-\mathrm{i}(\omega_2^0 t_2 + \omega_1^0 t_1^T)} F_{(t_2, t_1^T)}\{\tilde{\Phi}(\Omega_1,\Omega_2)\}, \tag{36}$$

where $F_{(t_2,t_1^T)}\{\tilde{\Phi}(\Omega_1,\Omega_2)\}$ is the previous mentioned Fourier transform of the JSA. Analogously, for the reflected component R we have:

$$\Psi_R(t_1^R, t_2) = \frac{\mathrm{i}}{2} e^{-\mathrm{i}(\omega_2^0 t_2 + \omega_1^0 t_1^R)} F_{(t_2, t_1^R)}\{\tilde{\Phi}(\Omega_2,\Omega_1)\}; \tag{37}$$

and for the interference term:

$$\Psi_T^* \Psi_R = \frac{1}{4} e^{-\mathrm{i}\omega_1^0 (t_1^R - t_1^T)} F^*_{(t_2, t_1^R)}\{\tilde{\Phi}(\Omega_1,\Omega_2)\} F_{(t_2, t_1^T)}\{\tilde{\Phi}(\Omega_1,\Omega_2)\}. \tag{38}$$

To obtain the explicit form of the JSA of the Eq. 26, we replace the functional form of the filters

$$\tilde{\Phi}(\Omega_1,\Omega_2) = \mathcal{N} \exp\left[-\alpha\Omega_1^2/2 + \beta\Omega_1\Omega_2 - \gamma\Omega_2^2/2\right], \tag{39}$$

where α, β and γ are [45]

$$\alpha = \frac{1}{2}\left(\frac{1}{\sigma_-^2} + \frac{1}{\sigma_+^2} + \frac{1}{\sigma_1^2}\right), \tag{40}$$

$$\beta = \frac{1}{2}\left(\frac{1}{\sigma_-^2} - \frac{1}{\sigma_+^2}\right), \tag{41}$$

$$\gamma = \frac{1}{2}\left(\frac{1}{\sigma_-^2} + \frac{1}{\sigma_+^2} + \frac{1}{\sigma_2^2}\right). \tag{42}$$

Looking again at Eq. 22, the next step is to integrate in time the square amplitudes we have just found. Starting with the non-interfering terms $\xi = R, T$ in Eqs. 36 and 37, we get

$$|\Psi_\xi(t_1^\xi, t_2)|^2 = \frac{1}{4}\left(\frac{\mathcal{N}}{\sqrt{\alpha\gamma - \beta^2}}\right)^2 \exp\left[-\frac{\alpha t_2^2 + 2\beta t_2 t_1^\xi + \gamma t_1^{\xi 2}}{(\alpha\gamma - \beta^2)}\right] \tag{43}$$

whose time integral is

$$\int dt_1^\xi dt_2 |\Psi_\xi(t_1^\xi, t_2)|^2 = \frac{\pi\mathcal{N}^2}{4\sqrt{\alpha\gamma - \beta^2}} \equiv R_0, \tag{44}$$

whereas the interference contribution gives

$$\int dt_1 dt_2 |\Psi_T^*(t_1^T, t_2)\Psi_R(t_1^R, t_2)| = R_0 \exp\left[-\frac{\gamma\ t^2}{4(\alpha\gamma - \beta^2)}\right], \tag{45}$$

where $t = t_1^T - t_1^R$ is the time delay due to the path difference in the interferometer arms, $\Delta L = ct$.

The final step to obtain R_c is to sum the non-interfering terms and the interfering one (Eq. 44 and Eq. 45) which appears in Eq. 31:

$$R_c = 2R_0 + 2\cos\omega_1^0 t R_0 \exp\left[-\frac{\gamma\ t^2}{4(\alpha\gamma - \beta^2)}\right] \tag{46}$$

$$= 2R_0\left(1 + \cos\omega_1^0 t \exp\left[-\frac{\gamma\ t^2}{4(\alpha\gamma - \beta^2)}\right]\right) \tag{47}$$

$$= 2R_0\left(1 + V\cos\omega_1^0 t\right), \tag{48}$$

where we have used the relation $\Re(e^{\mathrm{i}\omega_1^0 t}) = \cos\omega_1^0 t$ appearing in Eq. 38. After normalization, the coincidence rate R_c becomes the quantum probability of Eq. 28.